# Investigating sources and sinks for ammonia exchanges between the atmosphere and a wheat canopy following slurry application with trailing hose

Erwan Personne, F. Tardy, Sophie Génermont, Celine Decuq, Jean Christophe Gueudet, Nicolas Mascher, Brigitte Durand, Sylvie Masson, Michel Lauransot, Christophe Flechard, et al.

Agricultural and Forest Meteorology 207 (2015) 11–23

Contents lists available at ScienceDirect

Agricultural and Forest Meteorology

journal homepage: www.elsevier.com/locate/agrformet

# Investigating sources and sinks for ammonia exchanges between the atmosphere and a wheat canopy following slurry application with trailing hose

Erwan Personne[a,*], Florence Tardy[b], Sophie Génermont[a], Céline Decuq[a], Jean-Christophe Gueudet[a], Nicolas Mascher[a], Brigitte Durand[a], Sylvie Masson[a], Michel Lauransot[a], Christophe Fléchard[c], Jürgen Burkhardt[d], Benjamin Loubet[b]

[a] UMR 1091 Environnement et Grandes Cultures, INRA-AgroParisTech, 78850 Thiverval-Grignon, France
[b] UR 26 Systèmes de culture à base de bananiers, ananas et plantains, CIRAD, Station de Neufchâteau, Sainte Marie, 97130 Capesterre-Belle-Eau, Guadeloupe FWI, France
[c] UMR 1069, SAS, INRA-AgroCampus Ouest, 65 Rue de Saint-Brieux, 35042 Rennes, France
[d] University of Bonn, Institute of Crop Science and Resource Conservation, Plant Nutrition Group, Karlrobert-Kreiten-Str. 13, 53129 Bonn, Germany

ARTICLE INFO

*Article history:*
Received 24 September 2014
Received in revised form
19 December 2014
Accepted 5 March 2015

*Keywords:*
Biosphere-atmosphere exchanges
Compensation point
Reactive nitrogen
Model
Fertilizer application
Field
Wheat

ABSTRACT

Ammonia exchanges between the atmosphere and terrestrial ecosystems are composed of several pathways including exchange with the soil, the litter, the plant surfaces (cuticle) and through the stomata. In this study, the fate of nitrogen in the different pools (soil and plant) was analyzed with the aim of determining the sources and sink of atmospheric ammonia after slurry application on a wheat canopy. To do this, we measured ammonia exchanges between a winter wheat canopy and the atmosphere following cattle slurry application with a trailing hose. From 12 March to 8 April in Grignon near Paris, France, the ammonia fluxes ranged from an emission peak of 54,300 $NH_3$ ng $m^{-2}$ $s^{-1}$ on the day of slurry application (with a median during the first 24 h of 5990 $NH_3$ ng $m^{-2}$ $s^{-1}$) to a deposition flux of −600 $NH_3$ ng $m^{-2}$ $s^{-1}$ (with a median during the last period of −16 $NH_3$ ng $m^{-2}$ $s^{-1}$). The ammonia compensation points were evaluated for apoplasm, foliar bulk, root bulk and litter bulk tissue, as well as for soil surface. Ammonia emission potentials defined by the ratios between the concentration in [$NH_4^+$] and [$H^+$] for each N ecosystem pool were in the same order of magnitude for the plant decomposed in apoplastic liquid, green leaf bulk tissue and cuticle, respectively, averaging at 73, 160 and 120; in green leaf bulk tissues, the emission potential decreased gradually from 230 to 78 during the period after slurry application, while in the dead leaf bulk tissues considered as litter, the emission potential reached a maximum of 50,200 after application stabilized at around 20000. The dynamic of the emission potential for roots was similar to the ammonium concentration in the first two centimeters of the soil, with a maximum of 820 reached two days after application and a minimum of 44 reached three weeks later. The surfatm-$NH_3$ model interpreted the emission and deposition fluxes by testing soil surface resistance. We conclude that emission of the first day application was driven by climatic conditions and ammonia concentration at the soil surface, with no surface resistance and with only soil surface emission potential. On the next three days, the ammonia emission originated from the soil surface with the growth of a dry surface layer inducing surface resistance and regulated by slurry infiltration. The following days need a more detailed description of soil surface processes and the integration of vegetation exchanges (stomatal and cuticle pathways), particularly in the last period, in order to explain the ammonia deposition.



## 1. Introduction

Since the discovery of the "Haber-Bosch process" (Howard and Rees, 1996), synthetic fertilizer production has increased the quantity of reactive nitrogen (Nr) dispersed in the environment, leading to a series of impacts, labelled collectively as the nitrogen cascade (Galloway et al., 2008). Reactive nitrogen accumulation in the environment is contributing to the acidification and eutrophication of ecosystems and the impaction of air quality and greenhouse gas balance (Sutton et al., 2011). One of the most mobile reactive nitrogen compounds is ammonia ($NH_3$) and its mobile ionic form ammonium ($NH_4^+$) which is mainly emitted by agriculture

* Corresponding author. Tel.: +33 1 30 81 55 70; fax: +33 1 30 81 55 63.
*E-mail address:* erwan.personne@agroparistech.fr (E. Personne).

http://dx.doi.org/10.1016/j.agrformet.2015.03.002

and especially livestock farming (Hertel et al., 2012; Webb and Misselbrook, 2004). Cultivated fields, especially after land spread manure, also emit ammonia (Sommer et al., 2003). Croplands can however be a source or a sink of ammonia, depending on the difference between the concentration above and within the canopy (Spirig et al., 2010; Sutton et al., 1993b). The $NH_3$ exchanges between the atmosphere and terrestrial ecosystems are composed of several pathways including exchange with the soil, the litter, the plant surfaces (cuticles) and through the stomata (Massad et al., 2010; Nemitz et al., 2004; Sutton et al., 2009). These exchanges always include equilibrium processes between the gaseous and the aqueous phase (the Henry equilibrium), and acid-base equilibrium either in the apoplast (Massad et al., 2008), in the water layer on the cuticles (Burkhardt et al., 2009; Flechard et al., 1999) or in the soil (Genermont and Cellier, 1997). For each compartment involved, a compensation point can be defined (soil, litter, apoplast, and cuticle). Several factors regulate stomatal fluxes such as plant metabolism, development stage, nitrogen status and climatic conditions (Massad et al., 2008). Factors impacting deposition on cuticles are the presence of liquid water on the cuticle and the pH of this water, which is itself dependent on the acid and basic compounds in this water layer (Burkhardt et al., 2009; Flechard et al., 2011).

Because of its complexity, the $NH_3$ exchange between terrestrial ecosystems and the atmosphere is still not very well parametrized in models, despite recent advances towards general schemes (Flechard et al., 2013; Massad et al., 2010). Comprehensive datasets including $NH_3$ fluxes as well as $NH_x$ content of each compartment of the ecosystems are required to improve our qualitative understanding and provide parametrization for the ammonia exchange models. This is especially true for bi-directional $NH_3$ exchanges over crops which have rarely been studied after fertilizer application (Bash et al., 2010; Cooter et al., 2010; Loubet et al., 2012; Walker et al., 2012). Measurements of $NH_3$ emissions using up-to-date methods over large fields are also required to validate $NH_3$ emission factors as there are doubts about early work on $NH_3$ emissions using small fields (Sintermann et al., 2012).

In order to properly understand the ammonia exchanges with the atmosphere, we analyzed the fate of the nitrogen in the different pools (soil and plant) with the objective of determining the sources and sink of atmospheric ammonia after slurry application on a wheat canopy. The focus was on the evolution of the concentrations of the different forms of nitrogen for the compartments potentially involved by this slurry application (soil and plant) and so investigating the origin of the key exchanges with the atmosphere.

The experiment took place near Paris during the stem elongation development stage. Apart from $NH_3$ fluxes and concentrations, the $NH_x$ and $NO_3^-$ content were measured in most compartments at several dates. Chemical compounds on the cuticles were also extracted and analyzed. The Surfatm-$NH_3$ model (Personne et al., 2009) was used to interpret the observations. Finally, the location, magnitude and temporal pattern of the sources and sinks of $NH_3$ in the canopy are discussed.

## 2. Materials and methods

### 2.1. Field site

The experimentation took place at the Grignon site (NitroEurope IP field site FR-Gri 48°51′N, 1°58′E) about 30 km west of Paris, France, from 12 March to 5 April 2012. The field was a 19 ha winter wheat crop (*Triticum aestivum* cv. Premio), located on a plateau with a gentle slope of 1%, sown on 20 October 2011 at a theoretical density of 230 seeds per $m^2$ (measured $126 \pm 23$). The soil type was a luvisol (loamy clay: 25% clay, 70% silt and 5% sand). The mean annual precipitation and temperature were 700 mm and 11.5 °C, respectively. The field was surrounded by other agricultural fields and a livestock farm approximately 500 m to the south–west (220–240 deg wind direction sector). Two kilometres further in the same direction was a waste incineration plant. During the experimentation, the main wind directions were north–west to south-west.

The field was managed with a maize/winter wheat/winter barley/or triticale, mustard or *Phacelia* rotation. The previous crop was maize which was harvested on 6 September 2011 and stalks left on the ground prior to reduced tillage and wheat seedling on 17 September 2011. This field has been managed with reduced tillage since 2000.

The field was fertilized on 13 March 2012 with cattle slurry using a trailing hose system at a target rate of 120 kg N $ha^{-1}$. On 23 March, a growth reducer, chlormequat chloride (2-chloroethyltrimethyl-ammonium chloride, $C_5H_{13}Cl_2N$) was applied at a rate of 0.92 kg $ha^{-1}$, which corresponds to a 90 g N $ha^{-1}$ and 413 g Cl $ha^{-1}$.

Soil, plants and slurry were sampled on three $10 \times 10$ m sampling plots before and after fertilization. These plots were chosen within a 50 m radius around the flux tower. The crop was at stem elongation (stage 5 on Feekes' scale, (Zadoks et al., 1974)) during the experiment. From 29 February to 26 March the crop grew from 0.15 m to around 0.30 m height and the leaf area index (LAI) increased from 0.45 to 1.2 $m^2$ $m^{-2}$.

### 2.2. Micrometeorological measurements

The three components of the wind velocity ($u$, $v$, $w$) and temperature ($T_{son}$) were measured using an ultrasonic anemometer (Gill Instruments Ltd., UK) at 50 Hz 3 m above the ground. The $CO_2$ and $H_2O$ concentrations were measured at 20 Hz with an open-path infra-red gas analyzer (Licor, Li-7500, USA) at the same height. The latent ($LE$) and sensible ($H$) heat fluxes were determined with the Eddy-covariance method. The $LE$ fluxes were corrected with the Webb Pearson Leuning method for the variations in air density due to heat and water vapour fluxes (Aubinet et al., 2000). An HMP-45 (Vaisala, FI) was used to record air temperature ($T_a$) and relative humidity (RH) at 3 m height. Global ($R_g$) and net ($R_n$) radiation were measured at 3 m height, respectively, with a pyranometer (CM7B Albedometer Kipp & Zonen, NL) and a pyrradiometer (NR-Lite, Kipp & Zonen, NL). The soil temperature ($T_{soil}$) was measured at 7 depths, with homemade copper-constantan thermocouples between 0 and 20 cm (0.5 cm, 2 cm, 5 cm, 10 cm, 20 cm) and with temperature probe (107, Campbell Sci. USA) at 30 and 90 cm. The soil water content (SWC) was recorded with TDR probes (CS616 time domain reflectometry, Campbell Sci. USA). Potential leaf wetness (DH) was measured with 237 wetness sensing grids (Campbell Sci. USA) and precipitations with an ARG 100 tipping bucket raingauge (Campbell Sci. USA). Full details of the micrometeorological measurements can be found in Loubet et al. (2011).

### 2.3. Ammonia concentrations and fluxes

Ammonia concentration was integrated during 30 min at 1.6, 0.75 and 0.4 m above ground using the ROSAA device (Robust and Sensitive Ammonia Analyzer, patent registration 10 55253, UCPI, France). The ROSAA analyzer is based on trapping atmospheric ammonia in a continuous flow of an 0.5 g $L^{-1}$ $H_2SO_4$ acid solution drained through three low-flow vertical glass wet denuders. The acid solution is then analyzed with a conductimeter equipped with a semi-permeable membrane for ammonia selectivity. A detailed description of the analyzer can be found in (Loubet et al., 2012). The calibration was performed with standard solutions varying from 50, 100, 250 and 500 μg $NH_4^+$ $kg^{-1}$ to 230, 530, 750 and 1000 μg $NH_4^+$ $kg^{-1}$ passed every 2 h. A quality control was performed by

means of 352 and 355 μg $NH_4^+$ $kg^{-1}$ standard solutions also passed every 2 h.

The $NH_3$ flux above the wheat crop was measured with the aerodynamic gradient method (Hicks et al., 1987) detailed in (Sutton et al., 1993a) and (Loubet et al., 2012):

$$F_{NH_3} = -k \times u_* \times \frac{\partial C_{NH_3}}{\partial[\ln(z-d) - \psi_H((z-d)/L)]} \quad (1)$$

where $u_*$ is the friction velocity (m $s^{-1}$), $d$ is zero plane displacement (m), $z$ is height above the ground surface (m), $L$ is the Monin–Obukhov length (m), $\psi_H$ is the stability correction function for heat and trace gases, and $k$ is von Karman's constant ($k = 0.41$). The flux $F_{NH_3}$ was obtained by linear regression between the $NH_3$ concentration ($C_{NH_3}$) and $\ln(z-d) - \psi_H((z-d)/L)$ over the three measurement heights as explained in (Loubet et al., 2012). By integrating Eq. (1), the concentration at 1 m above $d$, ($C_{NH3}$ (1 m)), was also estimated.

### 2.4. Slurry application and composition

The trailing hose system consisted of 50 hoses attached to a metal bar adjusted to the wheat row size and splashed slurry from a height of 20 cm.

To determine the quantity of slurry intercepted by the crop, above-ground plants were sampled in 3 plots (0.0625 $m^2$) during the first 4 h after fertilization. The plant samples were put in 2 L nalgene bottles filled with 1 L of 0.5 M KCL solution. Nalgene bottles were weighed before and after addition of plant samples and were shaken for 30 min with a magnetic stirrer. After settling, liquid was retrieved, centrifuged and analyzed to determine total ammonia-N (TAN) concentration with an $NH_3$ analyzer (FloRRia Mechatronics, The Netherlands). Plant samples were recovered, washed with water then dried at 80 °C and weighed.

The slurry application volume was determined 3 times at 5 different random positions placed in the field, under the trailing hose system during application by collecting slurry in plastic vats (0.033075 $m^2$).

To analyze the slurry chemical composition, slurry was sampled 3 times during slurry application, at 10 h, 13 h, and 16 h T.U. in 10 L buckets then frozen at −18 °C prior to analyzes. Three sub-samples were taken from each bucket and analyzed at the soil analysis lab (LAS–INRA, Arras, France) for dry matter, pH, mineral nitrogen, organic carbon, total nitrogen, $NO_3$ and $NH_x$. A sub-sample (40 g) was analyzed for moisture and another (10 g) for residual moisture for a sample dried in ambient air. A sub-sample of the sample dried in ambient air (10 g) was used for pH measurement after being put in suspension in water. Mineral nitrogen ($NO_3^-$ and $NH_4^+$) was analysed, respectively, according to Griess-Ilosvay method (Keeney and Nelson, 1982) and Berthelot method (Krom, 1980) using spectrophotometric determination on a sub-sample of 60 g of fresh sample after extraction from a 0.5 mol $L^{-1}$ KCl solution. On a last sub-sample (50 g) organic carbon and total nitrogen were analyzed according to the Dumas method.

### 2.5. Soil and plant sampling and analysis

Plant and soil were sampled one day before fertilization, the day of fertilization and 1, 2, 3, 7, 14 and 21 days after the slurry application.

Three soil samples were taken with a soil auger from random locations on each of the three sampling plots for depths 0–2 cm, 2–15 cm and 15–30 cm, and frozen at −18° C prior to being analyzed by the soil lab analysis (LAS–INRA, Arras, France) with the same methods as for slurry. In each of the three plots, 15 green leaves, dead/yellow leaves (>50% yellow) and roots were sampled in two rows over 1 m.

Later, as the yellow leaves disappeared, only dead leaves with 100% yellow/brown blades were sampled and considered as litter. In fact, these dead leaves were dry and appeared totally disconnected from the plant functioning, easily detachable from the plant.

Green leaves were used for extraction of apoplastic and foliar bulk tissue solutions, yellow and dead leaves for foliar bulk tissue solution extraction and roots for root bulk tissue solution extraction. In the extracted solutions, pH, $NH_4^+$, $NO_3^-$ and total N and C were measured.

#### 2.5.1. Extraction of apoplastic solution

A modified version (Massad et al., 2009a) of the vacuum infiltration technique of (Husted and Schjørring, 1995) was used for extracting apoplastic solution. The sub-sample of green and developed leaves was washed with de-ionised water, blotted dry and weighed. Then leaves were put in a 60 mL syringe with 40 mL of indigo carmine solution. This solution, which does not have a significant effect on pH or $NH_4^+$ (Hill et al., 2001), was infiltrated for 5 min with 5 cycles of vacuum and pressure. Infiltrated leaves were carefully dried with laboratory paper and weighed. The apoplastic solution was then obtained by centrifugation at 2000 *g* for 10 min. The dilution of apoplastic solution by the indigo carmine solution was measured using a spectrophotometer at wavelength 595 nm (iEMS reader, Labsystems). The pH was measured before the sample was frozen in liquid N and stored at −18 °C before further analysis.

The centrifugation force and duration were determined after cytoplasm contamination tests on wheat leaves. These contamination tests consisted in measuring the activity of malate dehydrogenase (MDH) in apoplast extract relative to foliar bulk tissue extract using a spectrophotometer at wavelength 340 nm (Husted and Schjørring, 1995). The contamination was 1.26 ± 0.22% of MDH activity in apoplast extracts relative to foliar bulk tissue extracts. After apoplastic extraction, the remaining leaves were used for foliar bulk tissue extraction.

#### 2.5.2. Extraction of foliar and root bulk tissue solution

Sub-samples of leaves or roots were washed with de-ionised water, dried with laboratory paper and ground in liquid N using a mortar. A sample (0.2 g) of the ground material was put in a 1.5 mL tube with 1 mL of de-ionised water and shaken for 15 min. The foliar bulk tissue solution was then extracted by centrifugation at 9000 *g* for 20 min. The supernatant was retrieved, and pH was measured prior to freezing the sample in liquid N and storing at −18 °C. The remaining ground material was weighed, oven-dried at 80 °C for 48 h and weighed again prior to fine grinding in a ball mill mixer (Retsch, Verder, France) for 3 min at 30 pulsations per second. The obtained powder was stored in Eppendorf cups at ambient air prior to N and C analyses.

#### 2.5.3. Plant analysis

The pH measurements of apoplastic, foliar bulk tissue and root bulk tissue solutions were made with a pH semi-micro electrode (InLab Micro, Mettler Toledo, Udorf, Switzerland). The $NO_3^-$ concentration and the total N and C contents were measured with the same method as for slurry and soils. The $NH_4^+$ concentration was determined using the same flow injection $NH_3$ analyzer as for slurry.

### 2.6. Calculation of the $NH_3$ compensation point

The $NH_3$ compensation point is the gaseous concentration at equilibrium with an adjacent $NH_x$ ecosystem pool ($\chi_{pool}$) at the soil surface, in the litter, in the sub-stomatal cavity and at the cuticle surface (see Section 3.9). It was calculated according to (Schjørring,

1997; Schjørring et al., 1998) based on thermodynamic equilibrium between aqueous and gaseous $NH_3$ and acid-base equilibrium between $NH_4^+$ and $NH_3$ in the solution (see e.g., Personne et al., 2009):

$$\chi_{pool} = \Gamma_{pool} \times K_d \times K_H \times \exp\left(\frac{\Delta H^0_H + \Delta H^0_d}{R} \times \left(\frac{1}{298.15} - \frac{1}{T_{pool}}\right)\right) \quad (2)$$

where $\chi_{pool}$ is in mol $L^{-1}$, $\Delta H^0{}_H$ and $\Delta H^0{}_d$ are the free enthalpies of volatilization (34.18 kJ $mol^{-1}$) and acid-base dissociation (52.21 kJ $mol^{-1}$), $R$ is the perfect gas constant (8.314 J $mol^{-1}$ $K^{-1}$), $T_{pool}$ the ecosystem pool temperature ($K$), $K_d$ the dissociation constant for the $NH_4^+$ $NH_3$ equilibrium at 25 °C ($10^{-9.25}$ mol $L^{-1}$), $K_H$ the Henry constant at 25 °C ($10^{-3.14}$). In Eq. (2), the ratio $\Gamma_{pool} = [NH_4^+]_{pool}/[H^+]_{pool}$ is dimensionless, independent of temperature and represents the $NH_3$ emission potential of soil, litter or plant compartments (root, substomatal cavity, cuticle), pools with subscript $s$, $l$, root, stom and cut). $\Gamma_{pool}$ was calculated for each sample and averaged for each compartment.

The canopy emission potential $\Gamma(z_0)$ was estimated from measured $NH_3$ flux, by inverting Eq. (2) and replacing $\chi$ by $C_{NH3}(z_0)$. $C_{NH3}(z_0)$ was itself estimated by integrating Eq. (1) from $z_0$ (the canopy roughness length) to 1 m above the displacement height $d$:

$$C_{NH3}(z_0) = C_{NH3}(1m) + \frac{F_{NH3}}{ku_*} \times \left[\ln(1/z_0) - \psi_H(1/L) + \psi_H(z_0/L)\right] \quad (3)$$

### 2.7. Atmospheric deposition on the cuticles

Atmospheric deposition on the cuticles was analyzed on 23 March, 30 March and 5 April by washing the leaves with de-ionised water. Three samplings were made in the morning and three others in the afternoon for each of these three days. For each sampling, six wheat leaves were collected and put in a Teflon PFA bag. The cut extremities of each leaf were left well outside the Teflon pocket to avoid any contamination with compounds from inside the leaves. Then 2.5 mL of de-ionised water was added in the pocket and the leaf was washed by gently pressurizing the bag by hand. The leaf was then removed from the pocket, and its length and width were measured to determine its area. Each successive 2.5 mL rinsing water was transferred into a 20 mL tube leading to a 15 mL sample for each sampling. The pH was measured prior to freezing in liquid nitrogen and storage at −18 °C. The samples were analysed for $NO_3^-$, $PO_4^{3-}$, $SO_4^{2-}$, $Cl^-$ by high performance liquid chromatography (HPLC) and for $Na^+$ by inductively coupled plasma atomic emission spectrophotometry (ICP-AES). The cuticle emission potential $\Gamma_c$ was calculated for each sample and averaged.

The number of wheat leaves and the quantity of de-ionised water used were chosen to obtain samples adapted to the analysis methods; preliminary tests were carried out to establish the sampling method which showed that more than 80% of $NH_4^+$ ions deposited on cuticle were removed after the first washing (data not shown).

### 2.8. Interpretation of $NH_3$ fluxes with the Surfatm–$NH_3$ model

To help interpret the complexity of the interactions between the ecosystem compartments (soil, litter, stomata, cuticle and canopy air space), the Surfatm–$NH_3$ model was used. The Surfatm–$NH_3$ is a one-dimensional model (Personne et al., 2009) calculating the $NH_3$ flux in terrestrial ecosystem by coupling a water and energy balance model with a two-layer $NH_3$ resistance analogue model which considers soil, stomatal and cuticular pathways. The Surfatm–$NH_3$ model was tested for a grassland canopy following cutting and fertilization with ammonium nitrate (Sutton et al., 2009), and calibrated over a triticale field in Grignon (Loubet et al., 2012). The stomatal and soil $NH_3$ emission potentials $\Gamma$ used in the model were interpolated in time between those measured during the campaign. As our measurement campaign took place in the same field as in Loubet et al. (2012) we used the same model parameters except for:

- The attenuation coefficient for wind speed $\alpha_u$, set to 2.2 (instead of 4.2), to account for the difference in canopy structure, and the soil roughness $z_{0soil}$ was fixed to 0.02 m.
- The stomatal conductance parameters which came from (Emberson et al., 2000) following the EMEP approach for spring wheat, only $g_{max}$ was modified and fixed at 500 m mol $m^{-2}$ $s^{-1}$.
- The soil surface resistance ($R_{ss}$), set to 0 the day of the slurry application because of the liquid application, and the next day fixed at half of the value calculated by the expression for the vapor soil-surface resistance (Choudhry and Monteith, 1988)

$$R_{ss} = \frac{\tau_s \times \Delta_{dry}}{p_s \times D_{H_2O}} \quad (4)$$

where $\tau_s$ is a soil tortuosity factor (dimensionless), $\Delta_{dry}$ is the dry soil thickness (m), $p_s$ is the soil porosity (dimensionless) and $D_{H_2O}$ is the molecular diffusion for water in air ($m^2$ $s^{-1}$).

After these two specific adaptations for the water soil surface resistance due to the slurry application, the soil surface resistance for water was calculated using the original Eq. (4).

- The $NH_3$ soil-surface resistance ($R_{NH3_{soil}}$) was estimated using two methods:

(1) Using an equation similar to that for water soil transfer resistance (Personne et al., 2009): $R_{NH3_{soil}} = R1 = R_{ss} \times \frac{D_{H_2O}}{D_{NH_3}}$; this approach assumes that $NH_3$ comes from the aqueous phase which is incorporated in the soil wet layer.

- To mimicking the behavior of the cuticular resistance which decreases with relative humidity, the soil resistance was made dependent on air relative humidity: $R_{NH3_{soil}} = R2 = \beta \times (100 - RH) R_{NH3_{soil}} = R2 = \beta \times (100 - RH)$, where RH is relative humidity at 3 m height, and $\beta$ is an empirical coefficient which was fitted to optimize the comparison between measured and modelled ammonia fluxes ($\beta$ = 45).

Finally, in order to evaluate the role of this resistance $R_{NH3_{soil}}$, a run was performed with $R_{NH3_{soil}} = R0 = 0$, in which the cuticular resistance was set to infinity to simulate emission by the soil only.

## 3. Results

### 3.1. Meteorological conditions

During the experimentation the air temperature varied from −1.1 °C to 21.8 °C with an average of 9.8 °C. Relative humidity ranged from 24% to 98% and averaged 70%. The period was quite dry, with sporadic rain events on 14, 15, 17 and 18 March as well as 3 and 4 April with a maximum of 5.4 mm daily precipitation on 18 March. The cumulated precipitation over the period was 10.6 mm. The wind speed averaged 2.1 m $s^{-1}$ and varied from 0 to 6.1 m $s^{-1}$. The soil water content at 30 cm depth stayed almost constant with an average of 30.7% while at 5 cm depth it decreased from 31.2% to 26.9% after the rain event on 18 March. Global radiation exceeded 300 W $m^{-2}$ each day except on 31 March (Fig. 1).

**Table 1**
Cattle slurry characteristics and application rates. DM stands for dry matter and FW for fresh weight.

| | | Slurry characteristics | | Application rates | |
|---|---|---|---|---|---|
| | *n* | Average ± standard deviation | | | |
| Application rate | 15 | 92.4 ± 37.2 | Mg (FW) ha$^{-1}$ | | |
| Dry matter | 7 | 59.1 ± 9.5 | g (DM) kg$^{-1}$ (FW) | 5.5 ± 3.1 | Mg (DM) ha$^{-1}$ |
| Organic C | 7 | 406 ± 5 | g C kg$^{-1}$ (DM) | 2.2 ± 1.3 | Mg C ha$^{-1}$ |
| Total N | 7 | 25.9 ± 1.7 | g N kg$^{-1}$ (DM) | 141 ± 89 | kg N ha$^{-1}$ |
| pH | 7 | 8.3 ± 0.3 | – | | |
| $NO_3^-$ | 7 | 5.7 ± 0.6 | mg N kg$^{-1}$ (DM) | 31 ± 21 | g N ha$^{-1}$ |
| $NH_4^+$ | 7 | 20.2 ± 1.1 | g N kg– (DM) | 110 ± 68 | kg N ha$^{-1}$ |

### 3.2. Cattle slurry application

The cattle slurry was applied in the field with an application rate of 92.4 Mg ha$^{-1}$ with a large heterogeneity (standard deviation = 37.2 Mg ha$^{-1}$; Table 1). The total ammoniacal nitrogen (TAN) content was 1.2 g $NH_3$–N kg$^{-1}$ of manure which represented a TAN application rate of 111 kg $NH_3$–N ha$^{-1}$. The pH of the slurry was 7.7 ± 0.1.

### 3.3. Ammonia concentrations and fluxes

The atmospheric $NH_3$ concentration at 1 m above *d* varied over the period from 0.8 to 552 μg $NH_3$ m$^{-3}$ (Fig. 2a). The maximal concentration was reached in the evening of the fertilization day (13 March 2012) with a mean concentration during the first 24 h of 218 μg $NH_3$ m$^{-3}$. The concentration then decreased until 19 March when the daily mean was 9 μg $NH_3$ m$^{-3}$. From 20 to 26 March the concentration ranged from around 20 to more than 100 μg $NH_3$ m$^{-3}$ and averaged 21.0 μg $NH_3$ m$^{-3}$, with a marked peak on 23 March. From 28 March to the end of the measurement campaign, ammonia concentrations did not exceed 50 μg $NH_3$ m$^{-3}$. The last week of the campaign exhibited lower concentrations averaging 7.6 μg $NH_3$ m$^{-3}$.

Ammonia flux varied from −2800 to 54,330 μg $NH_3$ m$^{-2}$ s$^{-1}$ with a mean of 798 ng $NH_3$ m$^{-2}$ s$^{-1}$ and a median of 31 ng $NH_3$ m$^{-2}$ s$^{-1}$ (Fig. 2b). The main emission peak was observed the day of slurry spreading with a median 5990 ng $NH_3$ m$^{-2}$ s$^{-1}$ observed over the first 24 h. The following six days also showed large $NH_3$ emission (median 679 ng $NH_3$ m$^{-2}$ s$^{-1}$) slowly decreasing to switch to the first observed deposition fluxes on 20 March. A one-week period of alternating high daily emissions and small night-time deposition was then observed until 26 March, with a median of 34 ng $NH_3$ m$^{-2}$ s$^{-1}$ over the period. The last period (>26 March) mainly showed deposition with a median flux of −16 ng $NH_3$ m$^{-2}$ s$^{-1}$.

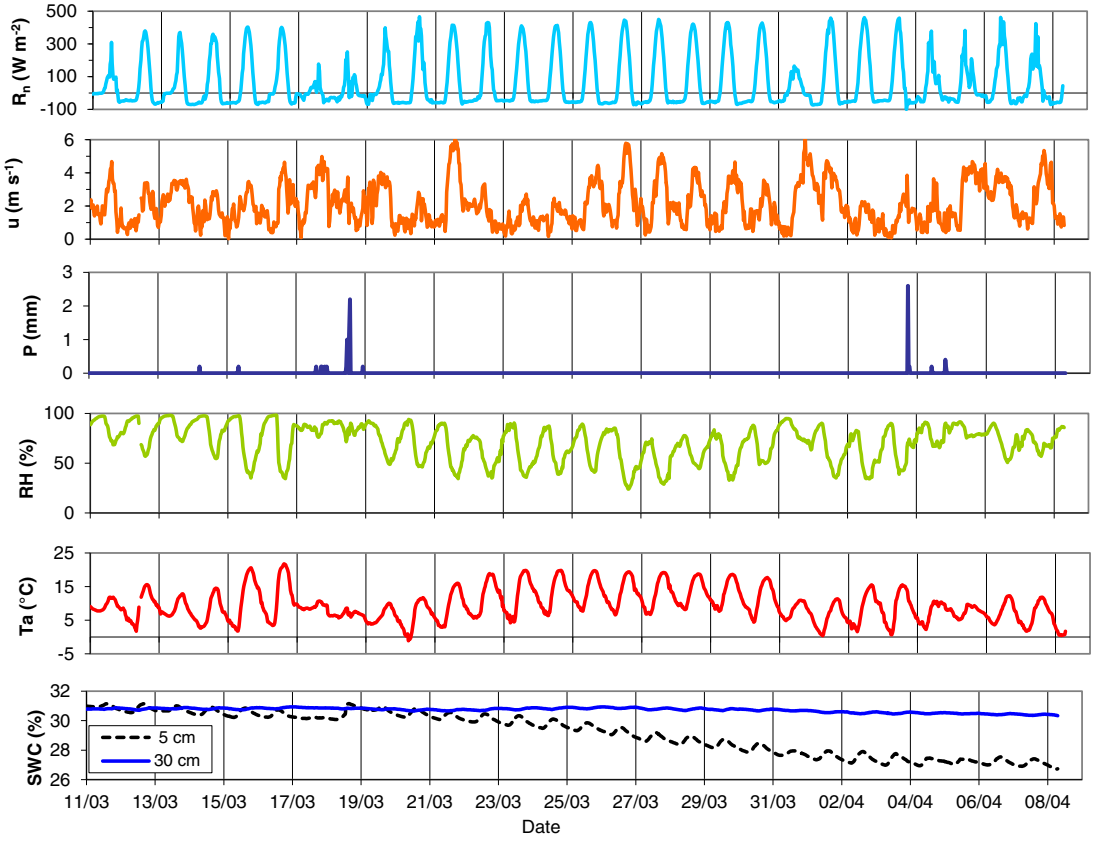


**Fig. 1.** Micrometeorological conditions measured at the site. From top to bottom: net radiation ($R_n$), wind velocity at 3 m height ($u$), precipitation ($P$), relative humidity (RH), air temperature ($T_a$) and soil water content (SWC) at 5 and 30 cm depth.

**Table 2**
Total ammonium nitrogen (TAN) applied, $NH_3$ lost by volatilization and emission factor.

| Period | Whole period kg N ha$^{-1}$ | 13/03–15/03 | 13/03–19/03 | 20/03–26/03 | 26/03–08/04 |
|---|---|---|---|---|---|
| Total applied nitrogen (TAN) | 110 | | | | |
| Cumulated $NH_3$ flux | 11.1 | 9.1 | 11.5 | 0.02 | −0.41 |
| Cumulated $NH_3$ emission | 12.9 | 9.1 | 11.5 | 1.06 | 0.35 |
| Cumulated $NH_3$ deposition | −1.8 | −0.01 | −0.01 | −1.04 | −0.76 |
| Emission factor (%) | 10.10% | 8.20% | 10.40% | 0.02% | −0.40% |

### 3.4. Cumulated volatilization and emission factor

The cumulated ammonia flux during the experimental period was 11.1 kg $NH_3-N$ ha$^{-1}$ which was composed of 12.9 kg $NH_3-N$ ha$^{-1}$ emission and −1.8 kg $NH_3-N$ ha$^{-1}$ deposition (Table 2). The emission factor was 10.1% of total ammoniacal nitrogen (TAN) applied (111 kg $NH_3-N$ ha$^{-1}$). Overall, 8.2% of $NH_3$ losses occurred during the first three days and 10.4% during the first week. The following week (20–26/03) 0.02% was lost, while afterwards 0.4% was deposited back to the canopy. During the first two weeks, most of the flux was towards emission, but during the last three weeks, the deposition term represented about 1 kg N ha$^{-1}$ (Table 2) and was included in the emission factor which did not decompose the sink and sources but quantified the balance.

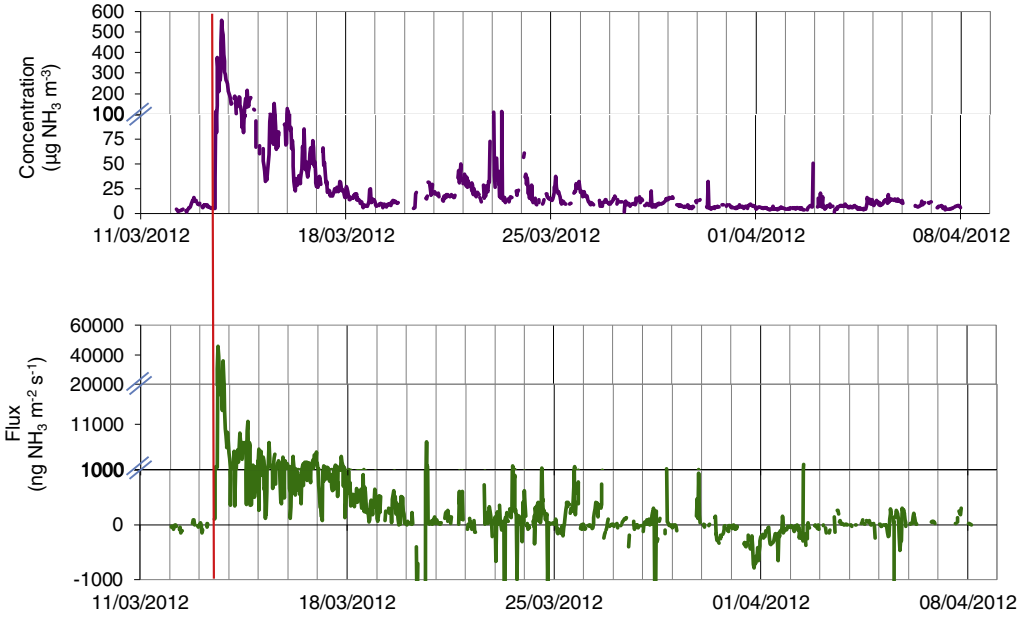


**Fig. 2.** Measured ammonia concentrations (a) and fluxes (b) above the wheat field. The vertical red line indicates time of fertilization. Two scales are shown for concentration and three for flux. Concentrations are expressed at 1 m above the displacement height.

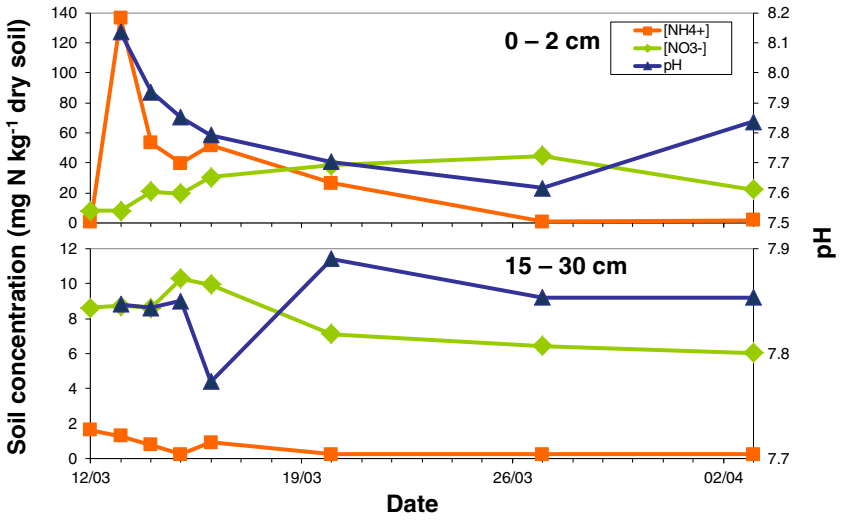


**Fig. 3.** Temporal variation in pH, [$NH_4^+$] and [$NO_3^-$] in the 2 cm top soil layer and the 15–30 cm layer. Slurry application was on 13 March.

**Table 3**
Emission potentials (Γ) in the different pools (plant, litter and soil) and at the canopy scale. Knowing measured $NH_3$ fluxes, $\Gamma_{z0}$ is estimated from Eq. (3) and $\Gamma_c$ is estimated as the intercept of the linear fit between the $NH_3$ flux and concentrations. Estimates in the soil layers 0–2 cm and 15–30 cm are also given together with estimates within or outside slurry bands.

| | | Plant | | | | Litter | Soil | | | | Canopy scale | |
|---|---|---|---|---|---|---|---|---|---|---|---|---|
| | | Apoplasm | Cuticle | Leaves | Roots | Litter | Mixed 0–2 cm | Mixed 15–30 cm | In slurry band 0–2 cm | Not in slurry band 0–2 cm | Γz0 | Γc |
| Whole period | Average | 73 | 120 | 160 | 340 | 29,000 | 1,700,000 | 24,000 | – | – | 161,000 | 2200 |
| | Std. dev. | 62 | 70 | 59 | 310 | 15,000 | 3,000,000 | 34,000 | – | – | 280,000 | 1700 |
| | Max | 110 | 200 | 230 | 820 | 50,000 | 5,800,000 | 178,000 | – | – | 650,000 | 5500 |
| | Min | 36 | 61 | 78 | 44 | 12,000 | 11,000 | 3000 | – | – | 4000 | 300 |
| 13–19/03 | Average | 88 | – | 170 | 610 | 43,000 | 3,300,000 | 35,000 | 7,300,000 | 430,000 | 409,000 | – |
| | Std. dev. | 73 | – | 40 | 280 | 11,000 | 4,100,000 | 42,000 | 6,700,000 | 860,000 | 423,000 | – |
| 20–27/03 | Average | 64 | 114 | 150 | 170 | 17,000 | 400,000 | 9000 | – | – | 33,000 | 3100 |
| | Std. dev. | 46 | – | 70 | 40 | 7000 | 600,000 | 4000 | – | – | 28,000 | 2400 |
| 30/03–05/04 | Average | 36 | 130 | 80 | 40 | 25,000 | 100,000 | 9000 | – | – | 9000 | 1200 |
| | Std. dev. | 60 | 97 | 80 | 40 | 25,000 | 100,000 | – | – | – | 9000 | 1000 |

**Table 4**
Quantity of ammonium, nitrate, phosphate, sulphate, chloride, and sodium on the leaves measured on the wheat leaf surfaces. The presence of dew on the leaves during sampling is also indicated. The $Cl^-$ content on the leaf was also expressed as percentage of the $Cl^-$ dose applied with the chlormequat chloride on 23 March (1165 μmol $m^{-2}$).

| Period | | $NH_4^+$ | $NO_3^-$ | $PO_4^{3-}$ | $SO_4^{2-}$ | $Cl^-$ | $Na^+$ | Total acids | Dew (obs.) | $Cl^-$ |
|---|---|---|---|---|---|---|---|---|---|---|
| | | μmol $m^{-2}$ (of leaf) | | | | | | | | % Appl. dose |
| 23/03/2012 | Morning | 30 ± 5.5 | 70 ± 34 | 21 ± 15 | 33 ± 4.5 | 648 ± 126 | 27 ± 0.4 | 772 ± 179 | +++ | 67% |
| | Afternoon | 12 ± 2.6 | 41 ± 11 | 10 ± 4.3 | 26 ± 4.6 | 479 ± 36 | 23 ± 0.7 | 556 ± 55 | ø | 49% |
| 30/03/2012 | Morning | 23 ± 6.9 | 53 ± 6.0 | 5.0 ± 1.6 | 33 ± 7.5 | 636 ± 145 | 12 ± 0.2 | 727 ± 160 | ++ | 65% |
| | Afternoon | 13 ± 2.7 | 45 ± 10 | 4.4 ± 0.6 | 25 ± 13 | 517 ± 188 | 12 ± 0.2 | 591 ± 211 | ø | 53% |
| 05/04/2012 | Morning | 13 ± 1.1 | 26 ± 8.5 | 2.1 ± 0.4 | 14 ± 4.6 | 310 ± 79 | 12 ± 0.2 | 351 ± 92 | ø | 32% |
| | Afternoon | 13 ± 0.6 | 24 ± 1.4 | 1.4 ± 0.5 | 12 ± 1.4 | 284 ± 95 | 13 ± 0.1 | 321 ± 98 | ø | 29% |
| 23/03/2012 | Daily | 21 ± 14 | 55 ± 30 | 15 ± 13 | 30 ± 6.5 | 563 ± 144 | 25 ± 2.2 | 664 ± 192 | – | 58% |
| 30/03/2012 | Daily | 18 ± 9.3 | 49 ± 12 | 4.7 ± 4.4 | 29 ± 7.6 | 576 ± 143 | 12 ± 8.4 | 659 ± 162 | – | 59% |
| 05/04/2012 | Daily | 13 ± 8.6 | 25 ± 10 | 1.7 ± 1.2 | 13 ± 11 | 297 ± 187 | 13 ± 0.4 | 336 ± 209 | – | 31% |
| Average | μmol $m^{-2}$ (of leaf) | 17 ± 11 | 43 ± 24 | 7.2 ± 9.4 | 24 ± 13 | 479 ± 223 | 17 ± 8.2 | 553 ± 269 | – | 49% |
| | g $ha^{-1}$ | 3.1 ± 1.5 | 21 ± 10 | 6.9 ± 7.8 | 23 ± 10 | 170 ± 68 | 3.8 ± 1.7 | 220 ± 96 | – | – |
| | mg $L^{-1}$ (solution) | 0.15 ± 0.06 | 1.0 ± 0.4 | 0.3 ± 0.3 | 1.1 ± 0.4 | 8.1 ± 2.8 | 0.2 ± 0.1 | 10 ± 4 | – | – |

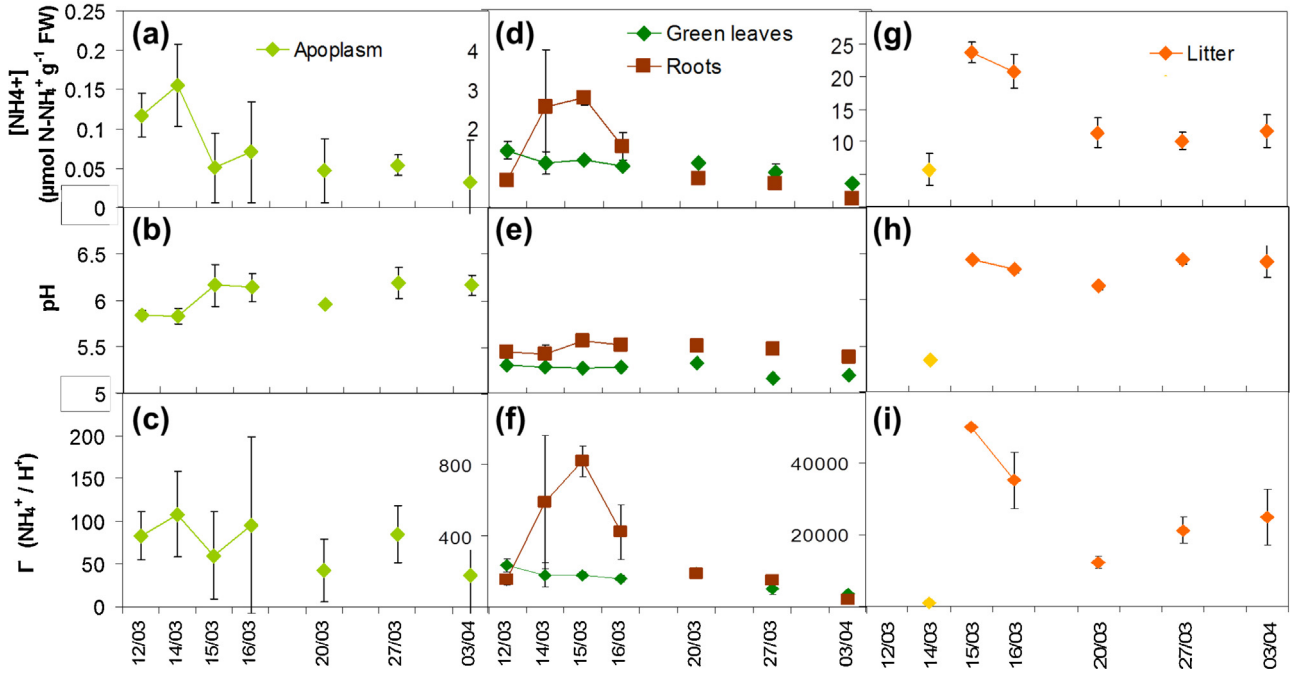


**Fig. 4.** Temporal variation in pH, $NH_4^+$ concentration and Γ in the apoplast, foliar bulk, root bulk, and litter bulk tissues ($\Gamma_{stom}$, $\Gamma_{green\text{-}leaves}$, $\Gamma_{roots}$, $\Gamma_{litter}$, respectively).

### 3.5. Ammonium nitrate and pH of the top soil

Concentrations of $NH_4^+$ and $NO_3^-$ as well as pH varied only in the top soil (0–2 cm) (Fig. 3). In this layer $NH_4^+$ concentration increased from 0.8 prior to fertilization to 136 mg N $NH_4^+$ $kg^{-1}$ on the day of fertilization. It more than halved the following day before decreasing to 0.9 mg N $NH_4^+$ $kg^{-1}$ in the third week of sampling. The $NO_3^-$ concentrations increased from 8.2 on the day following slurry spreading to 44.6 mg N–$NO_3^-$ $kg^{-1}$ on 27 March. It then decreased to 22.1 mg N $NO_3^-$ $kg^{-1}$ on 3 April. The soil pH decreased from 8.1

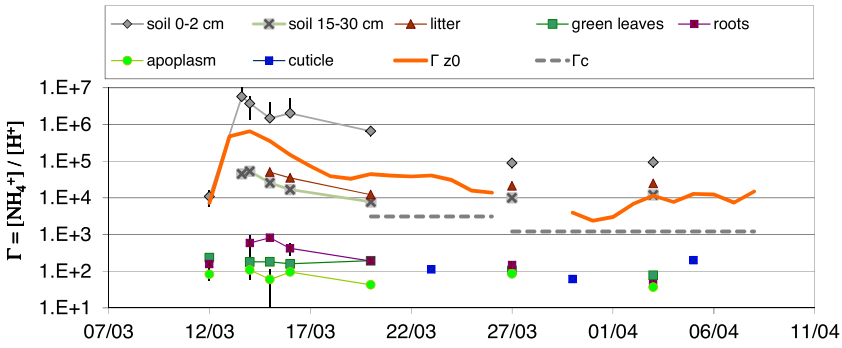


**Fig. 5.** Temporal variation of the Γ ratios ($[NH_4^+]/[H^+]$) measured in apoplastic solution, foliar bulk tissue, root bulk tissue, litter, soil in two layers, on cuticles and evaluated at $z_0$ from flux measurements. Measured Γ represent means of three replicates ± standard deviation, while $\Gamma_{z0}$ are daily averages.

to 7.6 but, as for $NH_4^+$ and $NO_3^-$ concentrations, the trend changed in the last week and the pH then rose.

### 3.6. Plant pools of ammonium, nitrate and pH

During the experimental campaign the apoplastic $NH_4^+$ concentration of green leaves varied from 0.15 to 0.03 μmol $NH_4^+$ $g^{-1}$ (FW) of leaf fresh weight, with a maximum reached on the day of fertilization (Fig. 4a). The apoplastic pH increased from 5.8 (12 and 14 March) to an average of 6.1 after 15 March (Fig. 4b). The foliar bulk tissues $NH_4^+$ concentration in green leaves decreased from 1.45 to 0.62 μmol $NH_4^+$ $g^{-1}$ (FW) (Fig. 4d) and in yellow leaves and litter varied from 5.7 to 23.7 μmol $NH_4^+$ $g^{-1}$ (FW) on the second day following slurry spreading (Fig. 4g). Bulk pH in green leaves remained constant during the 12–20/03 period and around fertilization at 5.3 (Fig. 4e). Yellow leaf and litter pH was higher and averaged 6.3 later than two days after nitrogen application (Fig. 4h). For both green leaves and yellow leaves in the bulk foliar tissues, the $NO_3^-$ concentration varied from 2.3 to 3.7 μmol $NO_3^-$ $g^{-1}$ (FW) without any visible trend (data not shown).

The root bulk tissue of wheat plants showed $NH_4^+$ concentrations increasing during the two days following fertilization to reach 2.8 μmol $NH_4^+$ $g^{-1}$ (FW); this root bulk tissue came back to its initial level around 0.6 μmol $NH_4^+$ $g^{-1}$ (FW) (Fig. 4d). On the other hand, the $NO_3^-$ concentration in roots decreased from 12 to 2 μmol $NO_3^-$ $g^{-1}$ (FW), while the pH remained constant and averaged 5.5 (Fig. 4e).

### 3.7. $NH_3$ emission potentials

The emission potential for the stomatal pathway, $\Gamma_{stom}$, averaged 73 over the whole period (Fig. 4c), and no significant trend could be observed during the period. In green leaves bulk tissues $\Gamma_{green\ leaves}$ decreased gently from 235 to 78 during the period (Fig. 4f) while in the dead leaves, bulk tissues considered as litter $\Gamma_{litter}$ reached a maximum of 50,200 on 15 March then stabilized to around 20,000 during the following weeks (Fig. 4i). In the roots, bulk tissues $\Gamma_{roots}$ were found to follow the same as the $NH_4^+$ concentration in the soil layer 0–2 cm, with a maximum of 820 reached on 15 March and a minimum of 44 reached three weeks later (Fig. 4f).

Ammonia emission potentials in the plant compartments (roots, leaves and apoplast) were all in the same order of magnitude during the whole experimental period, from 60 to 1000 (Fig. 5). On the other hand, the emission potential for the yellow leaves or litter leaves ($\Gamma_{litter}$) was roughly a hundred times larger than for plant, and the soil emission potential ($\Gamma_{soil}$) was again a hundred times larger than $\Gamma_{litter}$ during the first week to reach 7 $10^6$ on the day of slurry application. Then $\Gamma_{soil}$ decreased to 1.1 $10^4$ on 27 March and increased again to $10^5$ the third week following slurry application. The calculated $\Gamma z_0$ was in between $\Gamma_{soil}$ and $\Gamma_{litter}$ during the campaign and varied from a maximum 6.5 $10^5$ after slurry application to 4 $10^3$ towards the end of March to increase again to around $10^4$ in April. The cuticle ammonia emission potential was only measured over three days. It was in the same order of magnitude as the plant emission potentials averaging 124. Finally, the compensation point of the canopy $\chi_c$ was also estimated as the atmospheric $NH_3$ concentration when the flux was changing sign. We obtained on average $\chi_c = 21.7 \pm 6.4$ μg $NH_3$ $m^{-3}$ during the 20–26 March period, and 8.5 ± 2.3 μg $NH_3$ $m^{-3}$ during the 28 March to 8 April period. Based on the averaged air temperature during these periods, a $\Gamma_c$ was estimated at 3140 and 1230 during these two periods (Fig. 3 and Table 3).

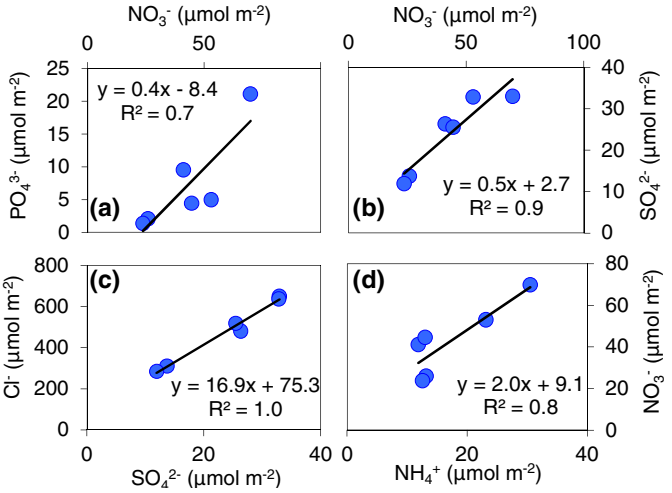


**Fig. 6.** Phosphate (a) and sulphate (b) versus nitrate. Chloride versus sulphate (c) and nitrate versus ammonium (d) surface. Content per leaf surface measured by washing wheat leaves on six dates. The linear regression line, equations and $R^2$ are also given.

### 3.8. Cuticular deposition

The concentrations of the different acid compounds and ammonium present on the leaves were higher in the morning than in the afternoon for the 23 March and 30 March (Table 4). They also showed different orders of magnitude: $PO_4^{3-}$ was in the order of 1–20 μmol $m^{-2}$ $NH_4^+$, $Na^+$ and $SO_4^{2-}$ were in the order of 12 to 33 μmol $m^{-2}$, $NO_3^-$ was in the order of 24–70 μmol $m^{-2}$ while $Cl^-$ was in the order of 284–648 μmol $m^{-2}$. The much higher $Cl^-$ concentration is explained by the application of chlormequat chloride (a growth reducer) on 23 March. Indeed the theoretical application rate of Cl was 413 g Cl $ha^{-1}$ which amounts to 1165 μmol $m^{-2}$. Accounting for the LAI which was measured as 1.2 $m^2$ $m^{-2}$ on 26

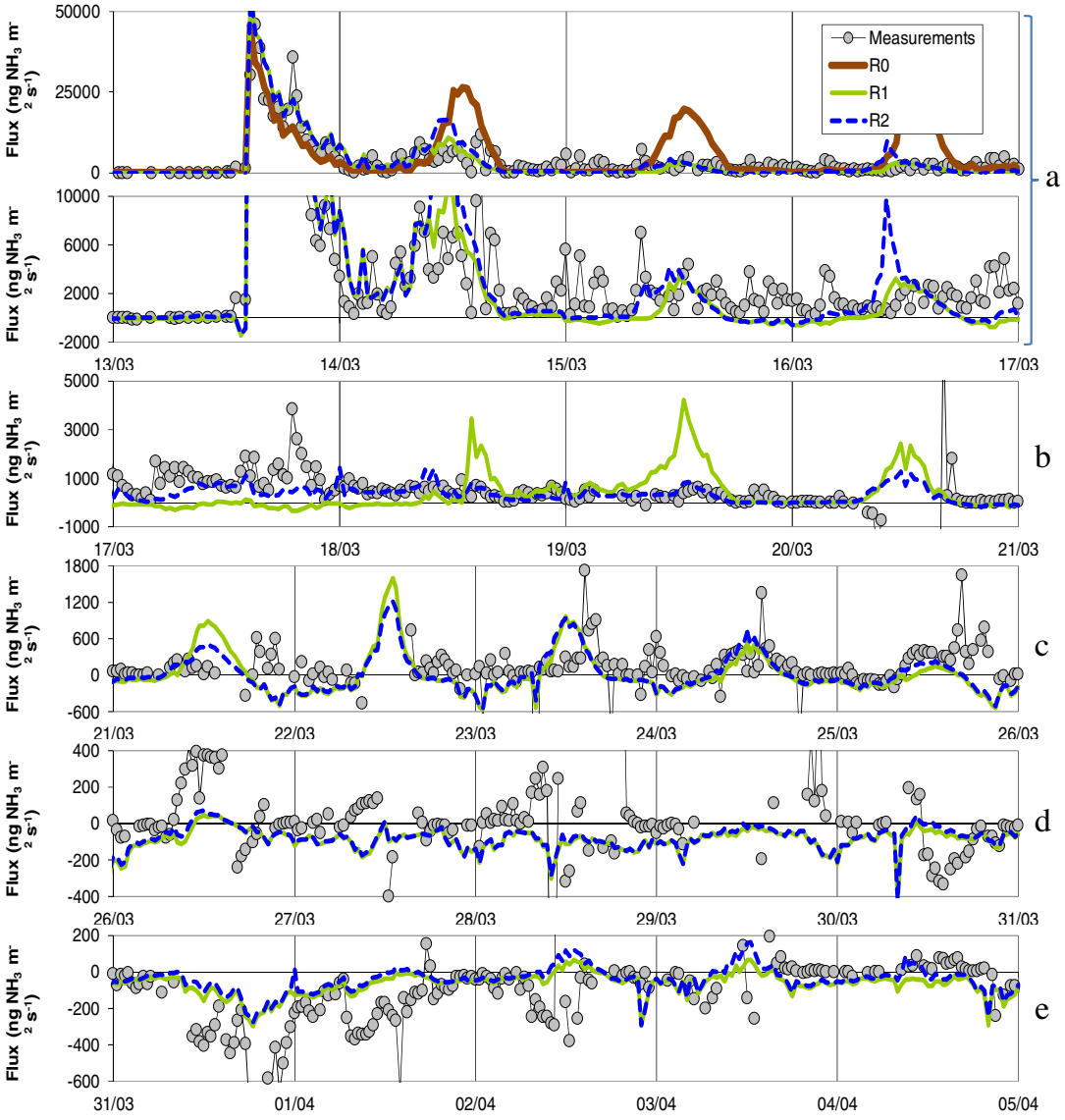


**Fig. 7.** Comparison of simulated and measured $NH_3$ fluxes with model parameterisation for the soil surface resistance $R_{NH3soil}$ = *R*0, *R*1 and *R*2 (see text). Each specific panel (from Fig. 7a–e) represents a sequence of four days; top two panels are for the same sequence. Every panel has its specific *y*-axis graduation in order to focus on the flux intensity.

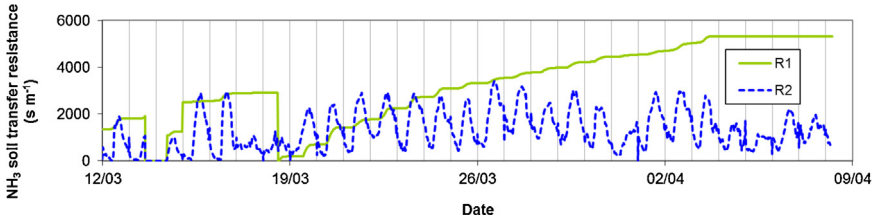


**Fig. 8.** Soil surface resistances for ammonia integrating in the SurfAtm model, *R*1 and *R*2; *R*1: similar to soil water resistance transfer; *R*2: mimicking the behavior of the cuticular resistance for ammonia, depending on relative air humidity.

March, the $Cl^-$ leaf surface content ranged from around 60% on the day of application and one week later, and down to 30% two weeks later.

A good relationship was found between $SO_4^{2-}$ and $Cl^-$ which suggests a similar depletion process for these two compounds but with a 20 times larger concentration for $Cl^-$. The nitrate content was also correlated to the ammonium content on the leaf surface with a slope equal to 2 (Fig. 6).

### *3.9. Comparison of the measured fluxes with the Surfatm–$NH_3$ model*

The stomatal and boundary layer resistances were tuned by changing $\alpha_u$ and $g_{max}$ (see §2.8) in order to get a correct evapotranspiration (LE) in the model. The calibrated model was well correlated with the measured LE:LE (model) = 1.001 LE (meas) + 2.06 (in W $m^{-2}$), with $R^2$ = 0.89 (data not shown). The mod-

elled sensible heat flux $H$ was compared to the measured energy balance default $H$(balance default) = Rn − LE − G (all measured) due to the fact that the measured energy balance does not close at this site (Loubet et al., 2011). The sensible heat and ground heat fluxes ($H$ and $G$) were also satisfactorily reproduced: $H$(model) = 0.813 $H$(balance default) − 1.97 (in W m$^{-2}$), $R^2$ = 0.90 and $G$(model) = 1.02 $G$(meas) − 2.72 (in W m$^{-2}$), $R^2$ = 0.62.

The modeled $NH_3$ flux with the soil emission potential $\Gamma_{soil}$ set to the measured values (interpolated) reproduced well the first peak of emission following fertilization but overestimated the measured flux the following days (Fig. 7a). However, with this parametrization the modeled nighttime fluxes were comparable to the measured values throughout the campaign. The modeled $NH_3$ flux obtained using the soil transfer resistance $R1$ for $NH_3$ agreed well with the measurements during the first two days following application (14 and 15/03), but not later. The use of the soil transfer resistance $R2$ with a resistance following the air relative humidity gave a reasonable agreement between modelled and measured $NH_3$ flux during the weeks following the first peak of emission, and during the period with alternating emissions and deposition from 22 to 26 March (Fig 7b and c). The last period of the survey (30 March to 8 April), during which a continuous deposition flux occurs, is quite well represented with the use of $R1$ or $R2$ resistances (Fig. 7e).

## 4. Discussion

### 4.1. Ammonium and pH in plant and litter pools

Ammonium concentrations were low in the plant tissues and apoplast (Fig. 4, Table 3). The apoplastic concentrations and Γ are similar to what (Mattsson et al., 1997) and (Husted and Schjørring, 1995) reported for Barley grown in chambers and (Mattsson et al., 2009; Loubet et al., 2002; Herrmann et al., 2009) for grasslands with no nitrogen application. Compared to the review of (Massad et al., 2009b), $\Gamma_{stom}$ is roughly three times lower than arable land receiving 150 kg N ha$^{-1}$, where $\Gamma_{stom}$ ∼300.

Regarding the dynamics of $NH_4^+$ concentration and Γ, we observed no response to fertilization of the apoplast and bulk tissue, which is in contradiction to (Mattsson et al., 2009; Loubet et al., 2002; Herrmann et al., 2009). Indeed, in a review, (Massad et al., 2010) (Fig. 6), showed that on average $\Gamma_{stom}$ increases to 1500 following a 100 kg N ha$^{-1}$ application. The root bulk tissue Γ increased up to 1000, while the litter bulk tissue increased by four orders of magnitude (40 000) following slurry application (Fig. 4). Mattson et al. (2009) also found a much higher Γ in senescent grassland leaves than in green leaves and stems, while (Morgan and Parton, 1989) reported an increase in whole plant compensation point at anthesis. Senescing leaves are not efficient sinks for nitrogen, therefore any incoming $NH_4^+$ will not be used as efficiently as in fast-growing leaves and may therefore accumulate, which would explain the observed increase in $NH_4^+$ in senescing leaves (Massad et al., 2008; Massad et al., 2010). This is supported by the fact that the Γ in the 15–30 cm soil layer (where the roots are located) was of the same order as in the litter leaves (Fig. 5).

Wheat crops and grassland have different nitrogen absorption regulation with a difference in the affinity for $NH_4$ and $NO_3$. Goyal and Huffaker (1986) reported a higher affinity for nitrate than ammonium in wheat. Also, large ammonium concentration may induce nitrate effluxes from roots as observed in cotton crops (Aslam et al., 2001). However, wheat roots can actively absorb $NH_4^+$, and can adapt quickly to $NH_4^+$ supply (Causin and Barneix, 1993). They can also efficiently absorb organic nitrogen such as amino acids (Gioseffi et al., 2012).

However, when compared to the grassland studies reported above (Mattsson et al., 2009; Loubet et al., 2002; Herrmann et al., 2009), a major difference is that nitrogen supply occurred following a grassland cut, while here the growth of the plant was uninterrupted. Cutting has two consequences: it induces a remobilization of nitrogen in the plant and hence $NH_4^+$ and it means that the nitrogen sink is less active in the plant. In our study the nitrogen sink was active and hence $NH_4^+$ which is an intermediate in the plant nitrogen cycle would not significantly increase (Massad et al., 2008, 2010a,b).

The wheat root depth did not have many roots in the top soil fraction 0–2 cm. At that stage the shoot-to-roots (5 cm depth) biomass ratio is indeed around 0.1 (Recous and Machet, 1999). Since the liquid manure did not greatly infiltrate the soil, as discussed in the next section, until the rainfall on 17 March, and since the high clay content of the soil led to high $NH_4^+$ immobilization on the clay fraction, it is likely that wheat plants did not absorb much $NH_4^+$ during that period. This is further likely because of the band application of slurry that would have led to a delay in root access to the N supplied in a similar manner as shown by (Petersen, 2005) for ammonium-nitrate: they measured a 5% m$^{-1}$ loss in maximum recovery of nitrogen and a 0.5 d cm$^{-1}$ increase in uptake. Since the inter-row was 16 cm, and the slurry band was roughly 5 cm in width, we can hypothesize a 25% loss in maximum recovery and a 2.5 day delay for the wheat to access the nitrogen. During that period, roughly 8% of the N was lost by volatilization leading to a further decrease in nitrogen accessible to the plant. Measurements of the soil $NH_4^+$ concentration outside the slurry band was indeed 6 times lower than that in the band and pH was also lower, leading to an emission potential (Γ) 17 time shigher in the band than outside (Fig. 3, Table 4).

Another explanation for the low response of green leaves $NH_4^+$ to slurry application is that soil was already rich in nitrogen and the wheat was not nitrogen-deficient. The total nitrogen measurements carried out on the green leaves at the beginning of the survey show a rate of 5% which is a high concentration for unfertilized young wheat plants (Barthes et al., 1996; Shangguan et al., 2004). The low uptake of the wheat could also be due to the young age of the crop at the fertilization date. (Limaux et al., 1999) showed that the amount of N uptake was positively linked to the crop growth rate; in our case the nitrogen application was early in the season and the crops may not have been sufficiently well-developed to absorb a large amount of nitrogen. Indeed, (Recous and Machet, 1999) have shown that theurea N uptake of wheat was the lowest for the period of application used in this study. Additionally, soil alkalinity due to the slurry would tend to lower N uptake (Wang et al., 2012).

We can conclude that we did not observe any increase in Γ in the growing plant compartments (excluding the senescing leaves) following slurry application, which is in contradiction to previous studies on grasslands but which might be consistent with the developmental stage of the wheat (small roots, fast growth), band application of slurry and growth of the wheat on rich cultivated soil. The observed increase in senescing leaves Γ following slurry application is consistent with existing studies and so it contributes to a pool of ammonia emission in the atmosphere (Fig. 5).

### 4.2. Ammonium and pH in soil pools

Ammonium concentration and pH in the top soil fraction (0–2 cm) increased dramatically with the nitrogen application then decreased quickly the day after and the following week. At the same time we noticed an increase of $NO_3^-$ concentration (Fig. 3). The pH of the top soil (8.1) was very close to the slurry pH (8.3) on the day of the application indicating a low, shallow infiltration, such as hypothesized by (Garcia et al., 2012). This is confirmed by the large difference observed in soil $NH_4^+$ and Γ between shallow infiltration

on and outside (Table 4, Figs. 3 and 5). Shallow infiltration would have led to a potential drying of the slurry at the soil surface, leading to physical nitrogen immobilization, until further decomposition or surface rewetting. The decrease in soil $NH_4^+$ concentration results from several processes: ammonia volatilization, ammonium nitrification, slurry infiltration, $NH_4^+$ transport and chemical equilibrium in the soil (Genermont and Cellier, 1997; Sommer et al., 2003). The top soil pH is expected to decrease. The top soil $NH_4^+$ concentration decreased towards its initial value after two weeks in response to $NH_3$ volatilization and $NH_4^+$ nitrification as reported by (Genermont et al., 1997; Sommer et al., 2003). Thompson and Meisinger (2004) observed a longer decay of one month in the 15 cm soil layer of a soil similar to this study. We can therefore conclude that the top soil $NH_4^+$ and $NO_3^-$ concentrations and pH measured following slurry application are in the range of reported studies, and that the slurry did not infiltrate the soil very deeply, leading to large $NH_3$ emissions and a quick decrease of $NH_4^+$ in the top soil. The $\Gamma$ soil obtained was high (Fig. 5, Table 3) in line with the large quantity of nitrogen applied and comparable to values reported by (Flechard et al., 2010) over grassland following cattle slurry application.

### 4.3. Cuticular deposition and chemical compounds on the cuticle

The ammonium content in the solution sampled on the cuticle was a factor of 10 lower than those reported by (Burkhardt et al., 2009) in dew and guttation on grassland leaves, which is consistent with the fact that we had to dilute the sample for collection, but which also shows that $NH_3$ deposition to grassland was probably larger (Table 4). However, we found similar $SO_4^{2-}$ and higher $NO_3^-$ content on the leaves when compared to (Burkhardt et al., 2009). This means that the acid to $NH_3$ deposition ratio was much higher in our study than in theirs. Finally we find a $Cl^-$ content which was a factor of 10 larger than theirs, which is explained by the application of chlormequat chloride on 23 March at a dose of 1165 $\mu$mol $m^{-2}$.

The cuticular emission potential ($\Gamma_{cut}$) was of the same order of magnitude as the $\Gamma_{stom}$ (Fig. 5) suggesting perhaps a continuity (passive transfer) between the inside and outside leaf solutions. A trans-cuticular transfer rate could be imagined, or a lateral migration flux in thin water films alongside stomatal guard cell surfaces. Ammonium deposed on leaf cuticles showed a variation of content between 23 March and 04 April and also between the morning and the afternoon: increasing the presence of water on the leaf surface is consistent with a larger deposition early in the experimental period and also early in the day (Burkhardt and Eiden, 1994; Burkhardt, 2009, Flechard et al., 1999). Other compounds measured on cuticles showed the same temporal variation; we assume there are some processes of co-deposition between acid compounds as suggested by (Sutton et al., 1995) and (Burkhardt et al., 2009).

### 4.4. Interpretation of the ammonia fluxes with the Surfatm–$NH_3$ model

The aim of using the Surfatm–$NH_3$ model was to question the exchange processes by trying to reproduce the measured flux with the model constrained by the measured stomatal, cuticular and soil emission potentials. The model was set up with measured $\Gamma_{stom}$ and $\Gamma_{soil}$ (0–2 cm) (Fig. 5), and two soil resistances were tested to account for the varying availability of $NH_3$ at the soil surface. While the first peak of emission was well reproduced with both soil-surface resistances, the model failed to reproduce the flux correctly during the following days if the surface resistance was set to 0 (case *R*0 in Fig. 7). This shows that ammonia was indeed available at the ground surface the first day but not after, confirming the assumption that the slurry did not infiltrate very deeply during the first day but it did so afterwards.

During the next three days, the model reproduced well the measured flux if the soil resistance for $NH_3$ was parametrized in a similar manner as for water vapor (Fig. 7a and b; *R*1 case). It can be supposed that a surface resistance takes place due to the ground surface drying.

However, to explain the representation of the first two weeks the assumption was that the resistance should be low during the night and higher during the day, like air relative humidity. The Surfatm simulated fluxes matched well with the measurements over the 15/03–27/03 period. *R*2 actually presents a daily variation which permits a regulation of the ammonia vaporization. It represents a mix process between mechanical surface resistance due to the drying process and $NH_4^+/NH_3$ availability in the aqueous film at soil surface.

Concerning the last period, we can suppose the 30/03–05/04 period was well represented because of the particularly low evaporation, the strong resistance (Fig. 8) and the low soil emission potential, favoring deposition fluxes.

As in Loubet et al. (2012) a very small minimal cuticular resistance was necessary to reproduce the largest deposition flux occurring on 31 March. As previously, some processes of co-deposition between acid compounds could be assumed, particularly due to the high chloride concentration on the leaves which seems to be persistent on the leaf surfaces.

The need to adjust surface resistance over time tested with the Surfatm–$NH_3$ simulations including only one soil water reserve; excluding soil physicochemical and biological processes suggests that processes such as infiltration, nitrification, nitrate leaching or organic matter adsorption need to be evaluated in order to better understand the ammonia exchanges following slurry applications.

### 4.5. Sources and sinks of $NH_3$ in the wheat canopy and ammonia emission factors

As described before we can observe different phases in the evolution of $NH_3$ flux. The first seven days are dominated by an emission flux then the second week is characterized by an alternation of emission and deposition fluxes. The last period of the experimentation is principally an ammonia deposition phase.

The first phase is explained by ammonia slurry volatilization, for the first day directly from slurry surface deposition, and then the principal source comes from the soil surface (Fig. 7a and b) and is driven by infiltration, surface drying and slurry physico-chemical properties. Then the variations of the second phase depend on the litter and soil sources (Fig. 7b and c), and probably due to physicochemical equilibrium with soil water and organic matter. The stomatal pathway is both source and sink, and we assumed it regulated the canopy ammonia balance. As Fig. 5 shows, soil and litter are the main drivers of the ammonia exchange in the canopy.

The 10.2% emission factor calculated over the whole experimental period (Table 4) is consistent with the results of (Bosch-Serra et al., 2014), (Meade et al., 2011), or (Martínez-Lagos et al., 2013), which report ammonia losses of between 6% and 18%, depending on the soil and climate conditions, although our ammonia losses are in the low range (Sintermann et al., 2012). Several elements are consistent to suggest that nitrogen losses in our experimental campaign are lower than other studies. First of all, the trailing hose for slurry application is a technique inducing lower emission than with splash plate application (Sintermann et al., 2012), then, the slurry application occurs during a cold period with a low air temperature (average temperature below 10 °C). This low temperature induces a low compensation point of the nitrogen pool (plant and soil) and so a low emission knowing that each increase of 5 °C lead to a doubling of the emission fluxes (Sommer et al., 2003). Finally, the measurement campaign took place on a soil with low-tillage inducing a soil structure that may be more favorable to infiltration

for slurry (no slaking). This soil is relatively carbonated and well-drained.The net ammonia emission rate is very high during the first 24 h with more than 50% of losses and close to 100% after 48 h.

## 5. Conclusions

The objective of the article was to examine the origins and magnitude of the ammonia exchanges between soil, plant and atmosphere after slurry application and how it changes day after day.

We conclude that the emission of the first day application is driven by climatic conditions and ammonia concentration directly obtained at the soil surface, without surface resistance and with only soil emission potential as key parameter. The three next days, the processes of ammonia emission from soil behave like soil evaporation, with the growth of a dry surface layer inducing surface resistance and regulated with slurry infiltration, suggesting that the biological and physicochemical processes are minor against mechanical transfer through the dry surface layer. The following phases need i/a more detailed description of the soil surface processes and ii/the integration of vegetation exchanges (stomatal and cuticle pathways), particularly in the last period.

Indeed, two weeks after slurry application, our experiment and simulation with Surfatm–$NH_3$ show that this period of alternation between emission and deposition fluxes is driven by the plant exchanges, either by the cuticle or by the stomatal absorption. During this last period, it can be observed that the chloride concentration on the leaves, due to chemical application of growth reducer, continued to be very high. This specific compound could explain the very low cuticular resistance explaining the high leaf deposition.

In parallel with this investigation, concerning the transfer of the nitrogen between the different pools (soil and plant) after slurry application, the plant compartments excluding senescing leaves had no evolution of their emission potential, probably due to nitrogen accessibility and/or to the young wheat plant growing on a soil without nitrogen deficiency and being itself without nitrogen deficiency.

Future works should be focused on:

- Coupling between biological and physicochemical nitrogen processes in the first soil centimeters and surface drying in order to evaluate the N availability for emission.
- Understanding nitrogen uptake by the growing plant depending on nitrogen soil content and soil properties.
- Physicochemical properties of the cuticle in order to better understand cuticle deposition and co-deposition.

## Acknowledgements

We gratefully acknowledge Dominique Tristan director of the AgroParisTech Farm for lending his field. This study was partially supported by a grant overseen by the French National Research Agency (ANR) as part of the “Investments d’Avenir” Programme (LabEx BASC; ANR-11-LABX-0034) and by EU-FP7 ECLAIRE, EU-FP7 INGOS, CASDAR “Volat’$NH_3$, ADEME “inventaires emissions spatialisés”, ADEME “caissons”.

## References

Aslam, M., Travis, R.L., Rains, D.W., 2001. Inhibition of net nitrate uptake by ammonium in pima and acala cotton roots. Crop Sci. 41, 1130–1136.

Aubinet, M., Grelle, A., Ibrom, A., Rannik, U., Moncrieff, J., Foken, T., Kowalski, A.S., Martin, P.H., Berbigier, P., Bernhofer, C., Clement, R., Elbers, J., Granier, A., Grunwald, T., Morgenstern, K., Pilegaard, K., Rebmann, C., Snijders, W., Valentini, R., Vesala, T., 2000. Estimates of the annual net carbon and water exchange of forests: the EUROFLUX methodology. Adv. Ecol. Res. 30 (30), 113–175.

Barthes, L., Deleens, E., Bousser, A., Hoarua, J., Prioul, J.L., 1996. Nitrate use and xylem exudation in detopped wheat seedlings: an early diagnosis for predicting varietal differences in nitrogen utilisation? Aust. J. Plant Physiol. 23, 33–44.

Bash, J.O., Walker, J.T., Katul, G.G., Jones, M.R., Nemitz, E., Robarge, W.P., 2010. Estimation of in-canopy ammonia sources and sinks in a fertilized *Zea mays* field. Environ. Sci. Technol. 44, 1683–1689, http://dx.doi.org/10.1021/es9037269.

Bosch-Serra À, D., Yagüe, M.R., Teira-Esmatges, M.R., 2014. Ammonia emissions from different fertilizing strategies in Mediterranean rainfed winter cereals. Atmos. Environ. 84, 204–212, http://dx.doi.org/10.1016/j.atmosenv.2013.11.044.

Burkhardt, J., Eiden, R., 1994. Thin water films on coniferous needles: a new device for the study of water vapour condensation and gaseous deposition to plant surfaces and particle samples. Atmos. Environ. 28, 2001–2011.

Burkhardt, J., Flechard, C.R., Gresens, F., Mattsson, M., Jongejan, P.A.C., Erisman, J.W., Weidinger, T., Meszaros, R., Nemitz, E., Sutton, M.A., 2009. Modelling the dynamic chemical interactions of atmospheric ammonia with leaf surface wetness in a managed grassland canopy. Biogeosciences 6, 67–84, http://dx.doi.org/10.5194/bg-6-67-2009.

Causin, H.F., Barneix, A.J., 1993. Regulation of $NH^{4+}$ uptake in wheat plants: effect of root ammonium concentration and amino acids. Plant Soil 151, 211–218, http://dx.doi.org/10.1007/BF00016286.

Choudhry, B.J., Monteith, J.L., 1988. A four-layer model for the heat budget of homogeneous land surfaces. Q. J. R. Meteorol. Soc. 114, 373–398.

Cooter, E.J., Bash, J.O., Walker, J.T., Jones, M.R., Robarge, W., 2010. Estimation of $NH_3$ bi-directional flux from managed agricultural soils. Atmos. Environ. 44 (juin 17), 2107–2115, http://dx.doi.org/10.1016/j.atmosenv.2010.02.044.

Emberson, L.D., Simpson, D., Tuovinen, J.P., Ashmore, M.R., Cambridge, H.M., 2000. Toward a Model of Ozone Deposition and Stomatal Uptake Over Europe. Norwegian Meteorological Institute, Oslo.

Flechard, C.R., Fowler, D., Sutton, M.A., Cape, J.N., 1999. A dynamic chemical model of bi-directional ammonia exchange between semi-natural vegetation and the atmosphere. Q. J. R. Meteorol. Soc. 125, 2611–2641.

Flechard, C.R., Massad, R.-S., Loubet, B., Personne, E., Simpson, D., Bash, J.O., Cooter, E.J., Nemitz, E., Sutton, M.A., 2013. Advances in understanding, models and parametrization of biosphere-atmosphere ammonia exchange. Biogeosci. Discuss. 10, 5385–5497, http://dx.doi.org/10.5194/bgd-10-5385-2013.

Flechard, C.R., Nemitz, E., Smith, R.I., Fowler, D., Vermeulen, A.T., Bleeker, A., Erisman, J.W., Simpson, D., Zhang, L., Tang, Y.S., Sutton, M.A., 2011. Dry deposition of reactive nitrogen to European ecosystems: a comparison of inferential models across the NitroEurope network. Atmos. Chem. Phys. 11, 2703–2728, http://dx.doi.org/10.5194/acp-11-2703-2011.

Flechard, C.R., Spirig, C., Neftel, A., Ammann, C., 2010. The annual ammonia budget of fertilised cut grassland – part 2: seasonal variations and compensation point modeling. Biogeosciences 7, 537–556.

Galloway, J.N., Townsend, A.R., Erisman, J.W., Bekunda, M., Cai, Z., Freney, J.R., Martinelli, L.A., Seitzinger, S.P., Sutton, M.A., 2008. Transformation of the nitrogen cycle: recent trends, questions, and potential solutions. Science 320, 889–892, http://dx.doi.org/10.1126/science.1136674.

Garcia, L., Génermont, S., Bedos, C., Simon, N.N., Garnier, P., Loubet, B., Cellier, P., 2012. Accounting for surface cattle slurry in ammonia volatilization models: the case of volt'air. Soil Sci. Soc. Am. J. 76, 2184, http://dx.doi.org/10.2136/sssaj2012.0067.

Genermont, S., Cellier, P., 1997. A mechanistic model for estimating ammonia volatilization from slurry applied to bare soil. Agric. For. Meteorol. 88, 145–167.

Gioseffi, E., de Neergaard, A., Schjoerring, J.K., 2012. Interactions between uptake of amino acids and inorganic nitrogen in wheat plants. Biogeosciences 9, 1509–1518, http://dx.doi.org/10.5194/bg-9-1509-2012.

Goyal, S.S., Huffaker, R.C., 1986. The uptake of $NO^{3-}$, $NO^{2-}$, and $NH^{4+}$ by intact wheat (*Triticumae stivum*) seedlings I. Induction and kinetics of transport systems. Plant Physiol. 82, 1051–1056.

Herrmann, B., Mattsson, M., Jones, S.K., Cellier, P., Milford, C., Sutton, M.A., Schjørring, J.K., Neftel, A., 2009. Vertical structure and diurnal variability of ammonia exchange potential within an intensively managed grass canopy. Biogeosciences 6, 15–23.

Hertel, O., Skjøth, C.A., Reis, S., Bleeker, A., Harrison, R.M., Cape, J.N., Fowler, D., Skiba, U., Simpson, D., Jickells, T., Kulmala, M., Gyldenkærne, S., Sørensen, L.L., Erisman, J.W., Sutton, M.A., 2012. Governing processes for reactive nitrogen compounds in the European atmosphere. Biogeosciences 9, 4921–4954, http://dx.doi.org/10.5194/bg-9-4921-2012.

Hicks, B.B., Baldocchi, D.D., Meyers, T.P., Hosker, R.P., Matt, D.R., 1987. A preliminary multiple resistance routine for deriving dry deposition velocities from measured quantities. Water. Air. Soil Pollut. 36, 311–330.

Hill, P.W., Raven, J.A., Loubet, B., Fowler, D., Sutton, M.A., 2001. Comparison of gas exchange and bioassay determinations of the ammonia compensation point in *Luzula sylvatica* (Huds.) gaud. Plant Physiol. 125, 476–487.

Howard, J.B., Rees, D.C., 1996. Structural basis of biological nitrogen fixation. Chem. Rev. 96, 2965–2982.

Husted, S., Schjørring, J.K., 1995. Apoplastic pH and ammonium concentration in leaves of *Brassica napus* L. Plant Physiol. 109 (December 4), 1453–1460.

Keeney, D.R., Nelson, D.W., 1982. Nitrogen: Inorganic forms. In Methods of soil analysis, Part 2. Chemical and microbiological properties. 2nd ed. In: Page A.L., (Ed.) Am. Soc. Agron. 9, 643–698.
Krom, M.D., 1980. Spectrophotometric determination of ammonia: a study of a modified Berthelot reaction using salicylate and dichloroisocyanurate. Analyst 105, 305–316.
Limaux, F., Recous, S., Meynard, J.M., Guckert, A., 1999. Relationship between rate of crop growth at date of fertiliser N application and fate of fertiliser N applied to winter wheat. Plant Soil 214, 49–59, http://dx.doi.org/10.1023/A.1004629511235.
Loubet, B., Decuq, C., Personne, E., Massad, R.S., Flechard, C., Fanucci, O., Mascher, N., Gueudet, J.-C., Masson, S., Durand, B., Genermont, S., Fauvel, Y., Cellier, P., 2012. Investigating the stomatal, cuticular and soil ammonia fluxes over a growing tritical crop under high acidic loads. Biogeosciences 9, 1537–1552, http://dx.doi.org/10.5194/bg-9-1537-2012.
Loubet, B., Laville, P., Lehuger, S., Larmanou, E., Flechard, C., Mascher, N., Genermont, S., Roche, R., Ferrara, R.M., Stella, P., Personne, E., Durand, B., Decuq, C., Flura, D., Masson, S., Fanucci, O., Rampon, J.-N., Siemens, J., Kindler, R., Gabrielle, B., Schrumpf, M., Cellier, P., 2011. Carbon, nitrogen and greenhouse gases budgets over a four years crop rotation in Northern France. Plant Soil 343, 109–137.
Loubet, B., Milfort, C., Hill, P.W., Tang, Y.S., Cellier, P., Sutton, M.A., 2002. Seasonal variability of apoplastic $NH^{+4}$ and pH in an intensively managed grassland. Plant Soil 238, 97–110.
Martínez-Lagos, J., Salazar, F., Alfaro, M., Misselbrook, T., 2013. Ammonia volatilization following dairy slurry application to a permanent grassland on a volcanic soil. Atmos. Environ. 80, 226–231, http://dx.doi.org/10.1016/j.atmosenv.2013.08.005.
Massad, R.-S., Loubet, B., Tuzet, A., Autret, H., Cellier, P., 2009a. Ammonia stomatal compensation point of young oilseed rape leaves during dark/light cycles under various nitrogen nutritions. Agric. Ecosyst. Environ. 133, 170–182, http://dx.doi.org/10.1016/j.agee.2009.04.020.
Massad, R.-S., Loubet, B., Tuzet, A., Autret, H., Cellier, P., 2009b. Ammonia stomatal compensation point of young oilseed rape leaves during dark/light cycles under various nitrogen nutritions. Agric. Ecosyst. Environ. 133, 170–182, http://dx.doi.org/10.1016/j.agee.2009.04.020.
Massad, R.S., Loubet, B., Tuzet, A., Cellier, P., 2008. Relationship between ammonia stomatal compensation point and nitrogen metabolism in arable crops: current status of knowledge and potential modelling approaches. Environ. Pollut. 154, 390–403, http://dx.doi.org/10.1016/j.envpol.2008.01.022.
Massad, R.-S., Nemitz, E., Sutton, M.A., 2010a. Review and parameterisation of bi-directional ammonia exchange between vegetation and the atmosphere. Atmos. Chem. Phys. 10 (10), 359–10386, http://dx.doi.org/10.5194/acp-10-10359-2010.
Massad, R.-S., Tuzet, A., Loubet, B., Perrier, A., Cellier, P., 2010b. Model of stomatal ammonia compensation point (STAMP) in relation to the plant nitrogen and carbon metabolisms and environmental conditions. Ecol. Model. 221, 479–494, http://dx.doi.org/10.1016/j.ecolmodel.2009.10.029.
Mattsson, M., Hausler, R.E., Leegood, R.C., Lea, P.J., Schjørring, J.K., 1997. Leaf-atmosphere $NH_3$ exchange in barley mutants with reduced activities of glutamine synthetase. Plant Physiol. 114 (August 4), 1307–1312.
Mattsson, M., Herrmann, B., David, M., Loubet, B., Riedo, M., Theobald, M.R., Sutton, M.A., Bruhn, D., Neftel, A., Schjørring, J.K., 2009. Temporal variability in bioassays of the stomatal ammonia compensation point in relation to plant and soil nitrogen parameters in intensively managed grassland. Biogeosciences 6, 171–179.
Meade, G., Lalor, S.T.J., Cabe, T.M., 2011. An evaluation of the combined usage of separated liquid pig manure and inorganic fertilizer in nutrient programmes for winter wheat production. Eur. J. Agron. 34, 62–70, http://dx.doi.org/10.1016/j.eja.2010.10.005.
Morgan, J., Parton, W., 1989. Characteristics of ammonia volatilization from spring wheat. Crop Sci. 29, 726–731.
Nemitz, E., Sutton, M.A., Wyers, G.P., Jongejan, P.A.C., 2004. Gas-particle interactions above a Dutch heathland: I. Surface exchange fluxes of NH(3), SO(2), HNO(3) and HCl. Atmos. Chem. Phys. 4, 989–1005.
Personne, E., Loubet, B., Herrmann, B., Mattsson, M., Schjorring, J., Nemitz, E., Sutton, M., Cellier, P., 2009. SURFATM-$NH_3$: a model combining the surface energy balance and bi-directional exchanges of ammonia applied at the field scale. Biogeosciences 6, 1371–1388.
Petersen, J., 2005. Inter-row crop competition for band-injected ammonium nitrate. Plant Soil 270, 83–90, http://dx.doi.org/10.1007/s11104-004-1169-4.
Recous, S., Machet, J.M., 1999. Short-term immobilisation and crop uptake of fertiliser nitrogen applied to winter wheat: effect of date of application in spring. Plant Soil 206, 137–149.
Schjørring, J.K., 1997. Plant-Atmosphere Ammonia Exchange: Quantification, Physiology Regulation and Interaction With Environmental Factors. R. Veterinary and Agric. Univ., Copenhagen, Denmark.
Schjørring, J.K., Husted, S., Mattsson, M., 1998. Physiological parameters controlling plant-atmosphere ammonia exchange. Atmos. Environ. 32 (February 3), 491–498, http://dx.doi.org/10.1016/S1352-2310(97)00006-X.
Shangguan, Z.P., Shao, M.A., Ren, S.J., Zhang, L.M., Xue, Q., 2004. Effect of nitrogen on root and shoot relations and gas exchange in winter wheat. Bot. Bull. Acad. Sin. 45, 49–54.
Sintermann, J., Neftel, A., Ammann, C., Haeni, C., Hensen, A., Loubet, B., Flechard, C.R., 2012. Are ammonia emissions from field-applied slurry substantially over-estimated in European emission inventories? Biogeosciences 9, 1611–1632, http://dx.doi.org/10.5194/bg-9-1611-2012.
Sommer, S.G., Génermont, S., Cellier, P., Hutchings, N.J., Olesen, J.E., Morvan, T., 2003. Processes controlling ammonia emission from livestock slurry in the field. Eur. J. Agron. 19, 465–486, http://dx.doi.org/10.1016/S1161-0301(03)37-6.
Spirig, C., Flechard, C.R., Ammann, C., Neftel, A., 2010. The annual ammonia budget of fertilised cut grassland – part 1: micrometeorological flux measurements and emissions after slurry application. Biogeosciences 7, 521–536.
Sutton, M.A., Fowler, D., Moncrieff, J.B., 1993a. The exchange of atmospheric ammonia with vegetated surfaces: I: unfertilized vegetation. Q. J. R. Meteorol. Soc. 119, 1023–1045.
Sutton, M.A., Nemitz, E., Milford, C., Campbell, C., Erisman, J.W., Hensen, A., Cellier, P., David, M., Loubet, B., Personne, E., Schjoerring, J.K., Mattsson, M., Dorsey, J.R., Gallagher, M.W., Horvath, L., Weidinger, T., Meszaros, R., Dämmgen, U., Neftel, A., Herrmann, B., Lehman, B.E., Flechard, C., Burkhardt, J., 2009. Dynamics of ammonia exchange with cut grassland: synthesis of results and conclusions of the GRAMINAE integrated experiment. Biogeosciences 6, 2907–2934, http://dx.doi.org/10.5194/bg-6-2907-2009.
Sutton, M.A., Oenema, O., Erisman, J.W., Leip, A., van Grinsven, H., Winiwarter, W., 2011. Too much of a good thing. Nature 472, 159–161, http://dx.doi.org/10.1038/472159a.
Sutton, M.A., Pitcairn, C.E.R., Fowler, D., 1993b. The exchange of ammonia between the atmosphere and plant communities. Adv. Ecol. Res. 24, 301–393.
Sutton, M.A., Schjorring, J.K., Wyers, G.P., 1995. Plant-atmosphere exchange of ammonia. Philos. Trans. R. Soc. London 351, 261–278.
Thompson, R.B., Meisinger, J.J., 2004. Gaseous nitrogen losses and ammonia volatilization measurement following land application of cattle slurry in the mid-Atlantic region of the USA. Plant Soil 266, 231–246.
Walker, J.M., Philip, S., Martin, R.V., Seinfeld, J.H., 2012. Simulation of nitrate, sulfate, and ammonium aerosols over the United States. Atmos. Chem. Phys. 12, 11213–11227, http://dx.doi.org/10.5194/acp-12-11213-2012.
Wang, Y., Zhang, F., Marschner, P., 2012. Soil pH is the main factor influencing growth and rhizosphere properties of wheat following different pre-crops. Plant Soil 360, 271–286, http://dx.doi.org/10.1007/s11104-012-1236-1.
Webb, J., Misselbrook, T.H., 2004. A mass-flow model of ammonia emissions from UK livestock production. Atmos. Environ. 38, 2163–2176.
Zadoks, J.C., Chang, T.T., Konzak, C.F., 1974. A decimal code for the growth stages of cereals. Weed Res. 14, 415–421, http://dx.doi.org/10.1111/j.1365-3180.1974.tb01084.x.